AAC Journals.ASM.org

Peptidyl Aldehyde NK-1.8k Suppresses Enterovirus 71 and Enterovirus 68 Infection by Targeting Protease 3C

Yaxin Wang,[a,d] Ben Yang,[b] Yangyang Zhai,[c] Zheng Yin,[c] Yuna Sun,[a] Zihe Rao[a,c,d,e]

National Laboratory of Macromolecules, Institute of Biophysics, Chinese Academy of Science, Beijing, China[a]; Phillips Academy, Andover, Massachusetts, USA[b]; College of Pharmacy & State Key Laboratory of Elemento-Organic Chemistry, Nankai University, and Collaborative Innovation Center of Chemical Science and Engineering (Tianjin), Tianjin, China[c]; University of Chinese Academy of Science, Chinese Academy of Science, Beijing, China[d]; Collaborative Innovation Center for Biotherapy, West China Hospital, West China Medical School, Sichuan University, Chengdu, China[e]

Enterovirus (EV) is one of the major causative agents of hand, foot, and mouth disease in the Pacific-Asia region. In particular, EV71 causes severe central nervous system infections, and the fatality rates from EV71 infection are high. Moreover, an outbreak of respiratory illnesses caused by an emerging EV, EV68, recently occurred among over 1,000 young children in the United States and was also associated with neurological infections. Although enterovirus has emerged as a considerable global public health threat, no antiviral drug for clinical use is available. In the present work, we screened our compound library for agents targeting viral protease and identified a peptidyl aldehyde, NK-1.8k, that inhibits the proliferation of different EV71 strains and one EV68 strain and that had a 50% effective concentration of 90 nM. Low cytotoxicity (50% cytotoxic concentration, >200 μM) indicated a high selective index of over 2,000. We further characterized a single amino acid substitution inside protease 3C (3C^{pro}), N69S, which conferred EV71 resistance to NK-1.8k, possibly by increasing the flexibility of the substrate binding pocket of 3C^{pro}. The combination of NK-1.8k and an EV71 RNA-dependent RNA polymerase inhibitor or entry inhibitor exhibited a strong synergistic anti-EV71 effect. Our findings suggest that NK-1.8k could potentially be developed for anti-EV therapy.

Enterovirus (EV) and coxsackievirus (CV), which belong to the *Picornaviridae* family, are the major causative agents of hand, foot, and mouth disease (HFMD) in the Pacific-Asia region (1). Young children are more susceptible to enterovirus and coxsackievirus infection (2, 3), but a recent case study reported that coxsackievirus also causes severe infectious diseases in adults (4). In particular, EV71 causes severe encephalitis, aseptic meningitis, pulmonary edema, acute flaccid paralysis, and myocarditis, which lead to high fatality rates (5, 6). Moreover, in August 2014, an emerging EV, EV68, caused mild to severe respiratory illnesses among 1,116 young children in the United States and was also associated with neurological infections (7, 8).

Both enterovirus and coxsackievirus belong to the *Enterovirus* genus, family *Picornaviridae* (9). The EV genome contains a single-stranded positive-sense polyadenylated RNA of approximately 7,400 nucleotides (10). Translation of the single open reading frame is initiated by ribosomes that use an internal ribosomal entry site located in the 5′ untranslated region (UTR) region of the viral genome and gives rise to a polyprotein of approximately 250 kDa (11–14). This polyprotein is further processed into four structural proteins (VP1 to VP4) to form the viral capsid and seven structural proteins (2A to 2C and 3A to 3D) by two viral proteases (2A and protease 3C [3C^{pro}]), together with a protease precursor, 3CD (15).

The most striking variation is that both EV71 and EV68 can infect the central nervous system and cause severe infection and death, but coxsackieviruses cannot. Although EV71 vaccines have been applied to prevent these diseases in clinical trials (16), no drug is clinically available to control the deadly symptoms caused by EV71 or EV68 infection (17). Preclinical research has identified large numbers of inhibitors targeting multiple processes of the EV71 replication cycle. For instance, an adenosine nucleoside analog (NITD008) inhibits RNA-dependent RNA polymerase activity in EV71 (18, 19), rupintrivir (AG7088) inhibits the function of EV71 3C^{pro} (6, 20, 21), and pleconaril, GPP3, and cyclosporine block the entry of enteroviruses and coxsackieviruses (22–24). However, none of these reported inhibitors have been able to be advanced to clinical therapeutics.

In this work, we screened our library containing a number of chemical compounds targeting viral proteases and identified a peptidyl aldehyde, NK-1.8k, that inhibited the proliferation of various strains of EV71, as well as one EV68 strain, in human (RD and 293T) and monkey (Vero) cell lines and that had the best 50% effective concentration (EC_{50}) of 90 nM among the compounds tested. We characterized the profile of EV71 resistance to the compound and demonstrated that the amino acid substitution conferring resistance occurs in the viral protease. The combination of NK-1.8k and NITD008 or GPP3 exhibited a strong synergistic anti-EV71 effect. Our findings suggest that this compound could potentially be developed for anti-EV therapy.

Received 9 January 2015 **Returned for modification** 9 February 2015
Accepted 13 February 2015

Accepted manuscript posted online 17 February 2015

Citation Wang Y, Yang B, Zhai Y, Yin Z, Sun Y, Rao Z. 2015. Peptidyl aldehyde NK-1.8k suppresses enterovirus 71 and enterovirus 68 infection by targeting protease 3C. Antimicrob Agents Chemother 59:2636–2646. doi:10.1128/AAC.00049-15.

Address correspondence to Zheng Yin, zheng_yin@nankai.edu.cn, or Yuna Sun, sunyn@moon.ibp.ac.cn.

Y.W. and B.Y. contributed equally to this article.

doi:10.1128/AAC.00049-15

MATERIALS AND METHODS

Cell lines and viruses. African green monkey kidney (Vero) cells (ATCC CCL-81), human rhabdomyosarcoma (RD) cells, and human embryonic kidney 293T cells were grown in Dulbecco's modified Eagle's medium (DMEM; Gibco) supplemented with 10% fetal bovine serum (FBS; Gibco) at 37°C in a humidified incubator with 5% CO_2.

Plasmids containing EV71 strain SK-EV006 (GenBank accession number AB469182.1) and EV71 strain SK-EV006 with a green fluorescent protein (GFP) reporter gene inserted into the genome (EV71-GFP) were donated by Satoshi Koike (Tokyo Metropolitan Institute of Medical Science) for the initial phenotype screening. A single-round reporter system [the EV71(FY)-Luc pseudotype virus system] with pseudotype EV71 containing plasmids pcDNA6-FY-capsid and pEV71-Luc-replicon lacking the P1 region was kindly supplied by Wenhui Li from the National Institute of Biological Sciences, Beijing, China. Plasmids containing human EV71 strains AnHui1 (GenBank accession number GQ994988.1) and BrCr (GenBank accession number U22521) were kindly provided by Bo Zhang and Hualin Wang, respectively, from the Wuhan Institute of Virology. The complete genome of EV68 prototypic strain Fermon CA62-1 (GenBank accession number AY426531) was chemically synthesized and was used to rescue living virus.

Inhibitors and reagents. Chemical compounds in our screening library and NITD008 (25) and GPP3 (23), which were used for the synergy studies, were synthesized. Stock solutions were prepared at a concentration of 10 mM in distilled water with dimethyl sulfoxide (DMSO) (final concentration, 0.1% [vol/vol]) and before use were diluted to different concentrations with DMEM containing 10% FBS.

A MEGAscript T7 high-yield transcription kit was purchased from Ambion. The TRIzol reagent and a SuperScript III first-strand synthesis system for reverse transcription-PCR (RT-PCR) were purchased from Invitrogen. A QuantiTect SYBR green RT-PCR kit was purchased from Qiagen. A cell viability and proliferation assay (WST-1) was purchased from Roche.

Virus titration. For EV71-GFP, virus titers were determined by measuring the level of GFP expression in RD cells infected with EV71-GFP. Briefly, the measurement was performed by seeding 3×10^4 RD cells per well in 96-well microtiter plates. After overnight culture, EV71-GFP was serially diluted 10-fold with DMEM containing 10% FBS (10^{-1}- to 10^{-8}-fold dilutions) and added to RD cells. The plates were then incubated at 37°C in 5% CO_2. After 3 to 4 days, the level of GFP expression was monitored using an epifluorescence microscope.

For living virus, virus titers were determined by endpoint dilution assays (EPDAs). Briefly, the titers were measured by seeding 3×10^4 RD cells per well in 96-well microtiter plates. After overnight culture, virus was serially diluted 10-fold with DMEM containing 10% FBS (10^{-1}- to 10^{-8}-fold dilutions) and added to the RD cells. The plates were then incubated at 37°C in 5% CO_2. Virus titers were determined after 3 to 4 days. The virus titer, expressed as the 50% tissue culture infective dose ($TCID_{50}$), was determined using EPDAs.

Preparation of EV71 pseudotype virus. The EV71 pseudotype virus [EV71(FY)-Luc] was produced by using the method developed as previously described (26). Briefly, the plasmid pEV71-Luc subgenomic replicon was linearized through digestion with the SalI restriction enzyme and was used as the template for RNA transcription. The EV71 replicon RNA transcripts were prepared *in vitro* using Promega MEGAscript kits. The pcDNA6-FY-capsid plasmid was transfected into 293T cells at 60 to 80% confluence. After 24 h posttransfection (hpi), EV71 subgenomic replicon RNA was then transfected using the Lipofectamine 2000 reagent (Invitrogen). The EV71 pseudotype virus was harvested at 24 h after RNA transfection with two freeze-thaw cycles. To quantify the EV71 pseudotype virus, the stocks were serially diluted 10-fold and incubated with RD cells for 24 h at 37°C. The cells were then harvested, and the luminescence was detected with a Bright-Glo luciferase (Luc) assay system according to the manufacturer's protocol (Promega). For the inhibition assay, the EV71 pseudotype virus was diluted to give a final concentration of 10^6 relative luminescence units (RLU) per well in a 96-well plate.

Phenotype screening. RD cells were seeded at 3×10^4 cells per well in 96-well microtiter plates. After overnight culture at 37°C in 5% CO_2, RD cells were treated with a gradient of concentrations of different compounds ranging from 0.045 to 100 μM. After 2 h, RD cells were infected with EV71-GFP at a multiplicity of infection (MOI) of 1. At 24 hpi, the level of GFP expression was monitored using an epifluorescence microscope.

Western blot analysis. RD cells were treated with NK-1.8k at concentrations ranging from 0.05 to 0.2 μM and lysed in a buffer containing (50 mM Tris-HCl, pH 8.0, 150 mM NaCl, 1% NP-40, 0.5% sodium deoxycholate, 0.1% sodium dodecyl sulfate [SDS], 2 mM EDTA, 1 mM $NaVO_4$, 10 mM NaF). The level of expression of the EV71 VP1 protein in the lysates was determined by a spectrophotometer. Proteins were separated by SDS-polyacrylamide gel electrophoresis (PAGE) and transferred to a nitrocellulose membrane (Millipore). These membranes were blocked with a 5% nonfat dry milk solution in Tris-buffered saline for 4 h, incubated with specific primary antibodies (catalog number ab36367; Abcam), and then subsequently incubated with secondary antibodies conjugated with horseradish peroxidase (HRP). Proteins were visualized by chemiluminescence using Clarity Western ECL substrate (Bio-Rad).

qRT-PCR. The reduction in the amount of the viral genome in host cells after treatment with one of the test compounds was determined using living EV71 and cells in a quantitative RT-PCR (qRT-PCR)-based assay. Briefly, 10^5 cells were seeded in each well of 24-well tissue culture plates with complete culture medium, and the plates were incubated at 37°C in 5% CO_2. The medium was then replaced with medium containing EV71 strain A, B, or C, as well as EV68 strain Fermon CA62-1, at an MOI of 1 and compounds serially diluted to concentrations ranging from 0.0039 to 2 μM in the presence of 10% FBS and 0.5% DMSO, respectively. After the cells were treated for 24 h, total cellular RNA was extracted with the TRIzol reagent using standard protocols. A quantitative RT-PCR assay (for GADPH [glyceraldehyde-3-phosphate dehydrogenase], the primer sequences were 5′-CCCACTCCTCCACCTTTGACG-3′ [forward primer] and 5′-CACCACCCTGTTGCTGTAGCCA-3′ [reverse primer]) was performed using a QuantiTect SYBR green RT-PCR kit (Qiagen, Valencia, CA) following the manufacturer's protocol. EVs and GADPH transcript levels were determined by the $\Delta\Delta C_T$ threshold cycle (C_T) method. The percent inhibition was calculated as follows: [1 − (average number of compound-treated cells)/(average number of control cells)] × 100. Each data point represents the average of three replicates in cell culture.

Inhibitory effect on different cells. In order to eliminate the differences between cells, the EC_{50}s for RD, Vero, and 293T cells were determined. RD (3×10^4 per well), Vero (2×10^4 per well), and 293T (3×10^4 per well) cells were seeded in 96-well plates and cultured at 37°C in 5% CO_2 overnight. Cells were treated with a gradient of dilutions of the different compounds ranging in concentration from 0.003 to 100 μM. EV71 Fuyang was added to 96-well plates at an MOI of 1. The RNA was detected by qRT-PCR after 24 hpi, and the EC_{50}s on different cells were calculated by the use of GraphPad Prism software.

Virus titers in supernatants. The levels of reduction of the virus titers in the supernatants were determined by EPDAs. Briefly, RD cells (3×10^5 per well) were cultured in a 24-well plate and incubated at 37°C under 5% CO_2. On the following days, RD cells were treated with serially diluted compounds at concentrations ranging from 0.0039 to 2 μM in the presence of 10% FBS and 0.5% DMSO. After 2 h, EV71 (Fuyang strain) at an MOI of 1 was used to infect the cells. The viruses in the supernatants of the wells containing each concentration were added to new 96-well plates and diluted from 10^{-1} to 10^{-8}. The cytopathic effect was observed in every well after 72 hpi. The $TCID_{50}$s were calculated by use of the Reed and Muench calculator.

Cytotoxicity. Cytotoxicity was measured by a WST-1-based cell proliferation assay using a cytotoxicity assay kit according to the manufacturer's protocol (catalog no. 05015944001; Roche, USA). Briefly, Vero cells

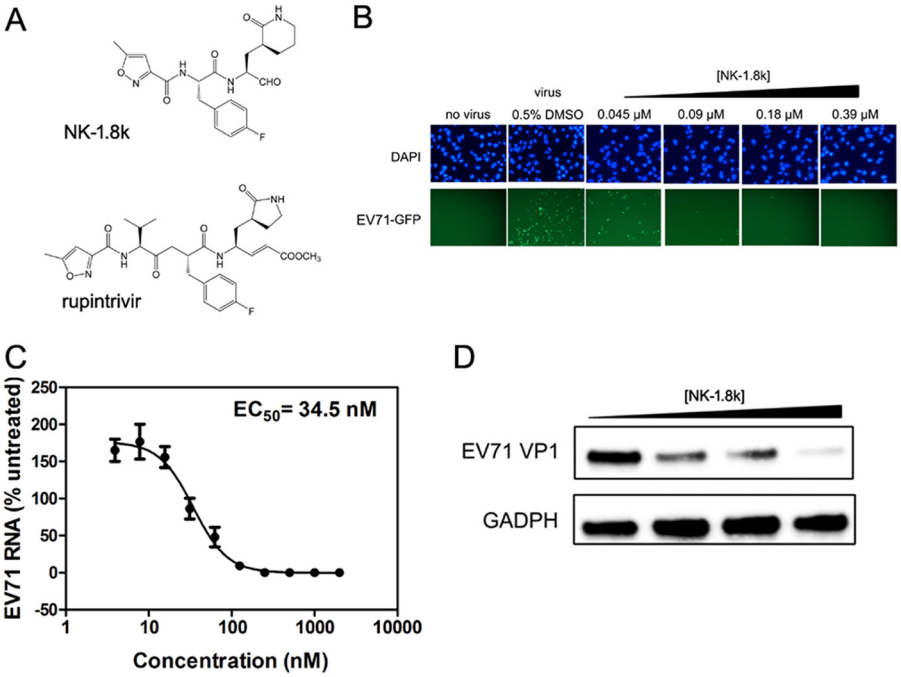

FIG 1 NK-1.8k inhibited EV71 proliferation. (A) Chemical structures of NK-1.8k and rupintrivir. (B) Concentration-dependent reduction of EV71 proliferation following treatment with NK-1.8k. RD cells were infected with EV71-GFP at an MOI of 1 and treated with various concentrations of NK-1.8k (0.045 to 0.39 μM) for 24 h or left untreated. DAPI (4′,6-diamidino-2-phenylindole) was used to visualize the nuclei (top) of the host cells, and enhanced GFP was used to monitor virus growth (bottom). (C) Inhibitory effect of NK-1.8k on EV71 RNA synthesis measured by qRT-PCR. RD cells were infected with EV71 at an MOI of 1 and treated with NK-1.8k at various concentrations (0.0039 to 2 μM) for 24 h or left untreated. Each point presents the average results from three independent experiments, and error bars represent SEMs ($n = 3$). (D) Dose-dependent reduction of EV71 VP1 expression. The concentration of NK-1.8k in the four lanes was 0.05, 0.1, 0.15, and 0.2 μM, from left to right, respectively. The level of GADPH expression was not affected by treatment with NK-1.8k.

(2×10^4 per well) and 293T and RD cells (3×10^4 per well in 100 μl 10% FBS–DMEM) were cultured at 37°C under 5% CO_2 in 96-well plates, followed by the addition of 50 μl of a solution containing each of the compounds to be tested at a concentration ranging from 0.78 to 200 μM. The cells were incubated at 37°C for 24 h, and then 10 μl WST-1 reagent was added to each well. The luminescent signals were read at 490 nm with a microplate reader (Bio-Rad, USA). The percentage of viable cells after treatment with different concentrations of compound was calculated as follows: percentage of viable cells = 100 × (OD_{490} of the treated sample/OD_{490} of the cell control sample), where OD_{490} is the optical density (OD) at 490 nm.

Time-of-addition assay. The time-of-addition effect was examined for NK-1.8k, NITD008, and GPP3. RD cells (3×10^4 cells per well in 100 μl 10% FBS–DMEM) were cultured overnight at 37°C under 5% CO_2 in 96-well plates. Subsequently, the cells were treated with 0.2 μM NK-1.8k, 2 μM NITD008, and 1 pM GPP3 either concurrently with 100 $TCID_{50}$s of EV71(FY)-Luc (0 h) or at intervals of −6, −4, −2, 0, 2, 4, 6, 8, and 10 hpi. Another 96-well plate was treated with NK-1.8k (0.2 μM), NITD008 (2 μM), and GPP3 (1 pM) and infected with EV71(FY)-Luc after 6 h. After incubation at 37°C for 24 h, antiviral activity was determined by measurement of the reduction of luciferase activity compared with the luciferase activity of the control cultures.

Selection of drug-resistant virus. RD cells were seeded at 6×10^5 cells/well in 6-well plates. On the following day, the medium was removed and replaced with DMEM containing 10% FBS and 0.2 μM NK-1.8k; 0.5% DMSO was used as a control. After 4 h, EV71 (Fuyang strain) was used to infect RD cells at an MOI of 0.1. After 3 days, the virus (termed passage 1 virus) was harvested when RD cells reached 70 to 90% confluence. A fresh 96-well plate was prepared and replaced with 0.2 μM NK-1.8k. RD cells were infected with EV71 at an MOI of 0.1, and virus from passage 2 was harvested. After three rounds of passage, the concentration of NK-1.8k was increased to 0.4 μM for another three rounds of passage and then to 0.8 μM for two rounds.

Identification of drug resistance-conferring mutations. For analysis of EV71 RNA resistance-conferring mutations, cellular RNA was extracted with the TRIzol reagent (Invitrogen) according to the manufacturer's instructions. For reverse transcription-PCR, first-strand cDNA was synthesized using a gene-specific primer (5′-ACCCCCACCAGTCA CATTCACG-3′) and the SuperScript III first-strand synthesis system for RT-PCR (Invitrogen) according to the manufacturer's instructions. The protein-coding region of the EV71 genome was amplified by PCR in 5 short fragments: fragment 1 was amplified with primers EV71-718-sense (5′-ATCTTGACCCTTAACACAGC-3′) and EV71-2046-anti (5′-GACC ATTGGGTGTAGTACCC-3′), fragment 2 was amplified with primers EV71-1975-sense (5′-CGATCCTGGGCGAAGTGGAC-3′) and EV71-3345-anti (5′-TGTTGTCCAAATT TCCCAAG-3′), fragment 3 was amplified with primers EV71-3248-sense (5′-TACCTATTCAAAGCCAA CCC-3′) and EV71-4643-anti (5′-ATAAAGACATATCCTTGCCG-3′), fragment 4 was amplified with primers EV71-4569-sense (5′-ACGGCTA CAAGCAACAGGTG-3′) and EV71-6044-anti (5′-TTCCCTCGAAGAT ATCATGG-3′), and fragment 5 was amplified with primers EV71-5972-sense (5′-GGAAGGCTCAACATCAATGG-3′) and EV71-7345-anti (5′-GGGTTGAGGTGTGTATAGCC-3′). The RT-PCR products of the 5 fragments of resistant EV71 or control EV71 were ligated into the TA cloning vector PMD18-T (TaKaRa). For each fragment, multiple individual bacterial colonies were isolated, and the purified plasmid DNA was sequenced. The sequences were aligned using Sequencher (version 5.0) and BioEdit software.

Sensitivity of EV71 WT and N69S mutant virus to NK-1.8k. The recombinant plasmid carrying EV71 (strain Fuyang) with a T7 promoter, a HindIII site before the 5′ UTR, and an XbaI site in the poly(A) sequence after the 3′ end was ligated into pcDNA 3.1. The N69S amino acid substi-

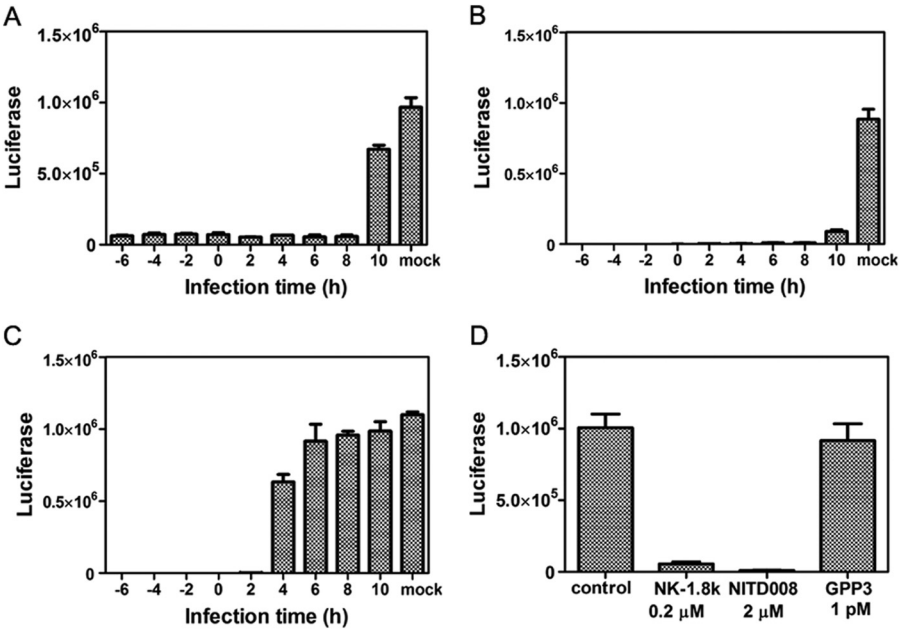

FIG 2 Anti-EV71 activities of NK-1.8k at different times of addition. (A to C) Inhibition of EV71(FY)-Luc pseudotype virus infection of RD cells by NK-1.8k (0.2 μM) (A), NITD008 (2 μM) (B), and GPP3 (1 pM) (C) at various times of addition. The luciferase levels at 24 hpi were quantified by measuring firefly luciferase activity in relative luminescence units (RLU). (D) EV71 subgenomic replicon RNA lacking the P1 region was transfected into RD cells treated with NK-1.8k (0.2 μM), NITD008 (2 μM), and GPP3 (1 pM) or left untreated (control). The luciferase levels were quantified at 24 hpi. Each point represents the average results from three independent experiments, and error bars represent SEMs ($n = 3$).

tution was generated by using a Fast mutagenesis system kit (Transgen) with forward primer 5′-ATGAGCAAGGAGTCAGCTTGGAATTAACC C-3′ and reverse primer 5′-CTGACTCCTTGCTCATCCACTAGCTCAA CTG-3′. The full-length RNAs of wild-type (WT) EV71 and the N69S mutant were transcribed from recombinant plasmid linearized with XbaI *in vitro* using a RiboMAX large-scale RNA production system (T7 kit; Promega). RD cells were electroporated with 10 μg of WT or mutant genome-length RNA. The WT and mutant viruses were harvested at 24 h posttransfection. RD cells (3×10^4 cells per well) were seeded in a 96-well plate and cultured at 37°C for 24 h. The WT and mutant virus titers were determined by EPDAs as described above. For testing the inhibitory activity of NK-1.8k between the WT and compound-resistant virus, 500 μl of the RD cell suspension was immediately seeded in a 24-well plate and the cells were incubated for 24 h. Cells were treated with serial dilutions of NK-1.8k and infected with WT or N69S virus. At 24 hpi, RNAs were extracted and quantify by qRT-PCR.

Interaction of NK-1.8k with other inhibitors of EV71 proliferation. The interaction of NK-1.8k and the other inhibitors was studied by use of a previously reported protocol and mathematical model, with some modifications (27, 28). Briefly, RD cells were seeded at 3×10^4 cells per well in 96-well microtiter plates. After an overnight culture at 37°C, a different final concentration of NK-1.8k (0, 0.3125, 0.0625, 0.125, 0.25, and 0.5 μM) was added to each row of the 96-well plate. Simultaneously, a different final concentration of NITD008 (0, 0.0625, 0.125, 0.25, 0.5, 1, 2, and 4 μM) was added to each column of the plate. RD cells were infected with the EV71 pseudotype virus after treatment with the two inhibitors and incubated for 24 h. The combination of NK-1.8k and GPP3 was tested by the same method, but with some adjustment. The concentrations of GPP3 used were 0.0005, 0.0019, 0.0078, 0.0312, 0.125, 0.5, and 2 μM. Antiviral activities were determined by measuring the reduction of luciferase activity in the cells.

Differential surface plots at the 95% confidence interval (CI) were calculated and generated by using the MacSynergy II program for the drug-drug interaction according to the Bliss independence model (28). The combination's effect was determined by subtracting the experimental values from the theoretical additive values (27, 28). In the three-dimensional differential surface plot, the peaks above and below a theoretical plane for additivity represent synergy and antagonism, respectively (27, 28). The data sets were interpreted as follows: volumes of synergy or antagonism with values of <25 mM^2% are insignificant, those with values of 25 to 50 mM^2% are minor but significant, those with values of 50 to 100 mM^2% are moderate and probably important *in vivo*, and those with values of >100 mM^2% are strong and likely to be important *in vivo*.

Protein production. Measurement of the production of EV71 WT, N69S mutant, and C147S mutant $3C^{pro}$ was based on a previously reported protocol (29–32). Briefly, the genomic region that codes for EV71 3C was amplified and cloned into the pET-28a vector (GE Healthcare) using the NdeI and NotI restriction sites. The recombinant plasmids were transformed into *Escherichia coli* strain BL21(DE3). Kanamycin-resistant colonies were grown in Luria-Bertani medium at 37°C until the OD_{600} reached 0.8. Isopropyl-β-D-1-thiogalactopyranoside was added to a final concentration of 0.5 mM, and the cultures were grown for an additional 20 h at 18°C. Cells were harvested by centrifugation, resuspended, and homogenized in lysis buffer containing 50 mM Tris-HCl (pH 7.0) and 200 mM NaCl, using a low-temperature ultra-high-pressure cell disrupter (JNBIO, Guangzhou, China). The lysate was centrifuged at 20,000 × *g* for 30 min to remove the cell debris. The supernatant was loaded onto an Ni-nitrilotriacetic acid affinity chromatography column (Qiagen). After washing with 50 mM Tris-HCl (pH 7.0), 200 mM NaCl, and 50 mM imidazole, the $3C^{pro}$ protein was washed with 50 mM Tris-HCl (pH 7.0), 200 mM NaCl, and 500 mM imidazole. The sample was further purified using a HiTrap S column (GE Healthcare) with a linear gradient of from 0 mM to 500 mM NaCl with 50 mM Tris-HCl (pH 7.0) and 2 mM dithiothreitol (DTT). The target proteins were concentrated to 12 mg/ml in a buffer with 20 mM Tris-HCl (pH 7.0), 500 mM NaCl, and 2 mM DTT for storage.

***In vitro* protease activity assay.** In the *in vitro* cleavage assay, the peptide was attached to a fluorescence-quenching pair of peptides, and the fluorogenic peptide NMA-IEALFQGPPK(DNP)FR (where NMA is *N*-methylanthranyl and DNP is dinitrophenol) was used as the substrate

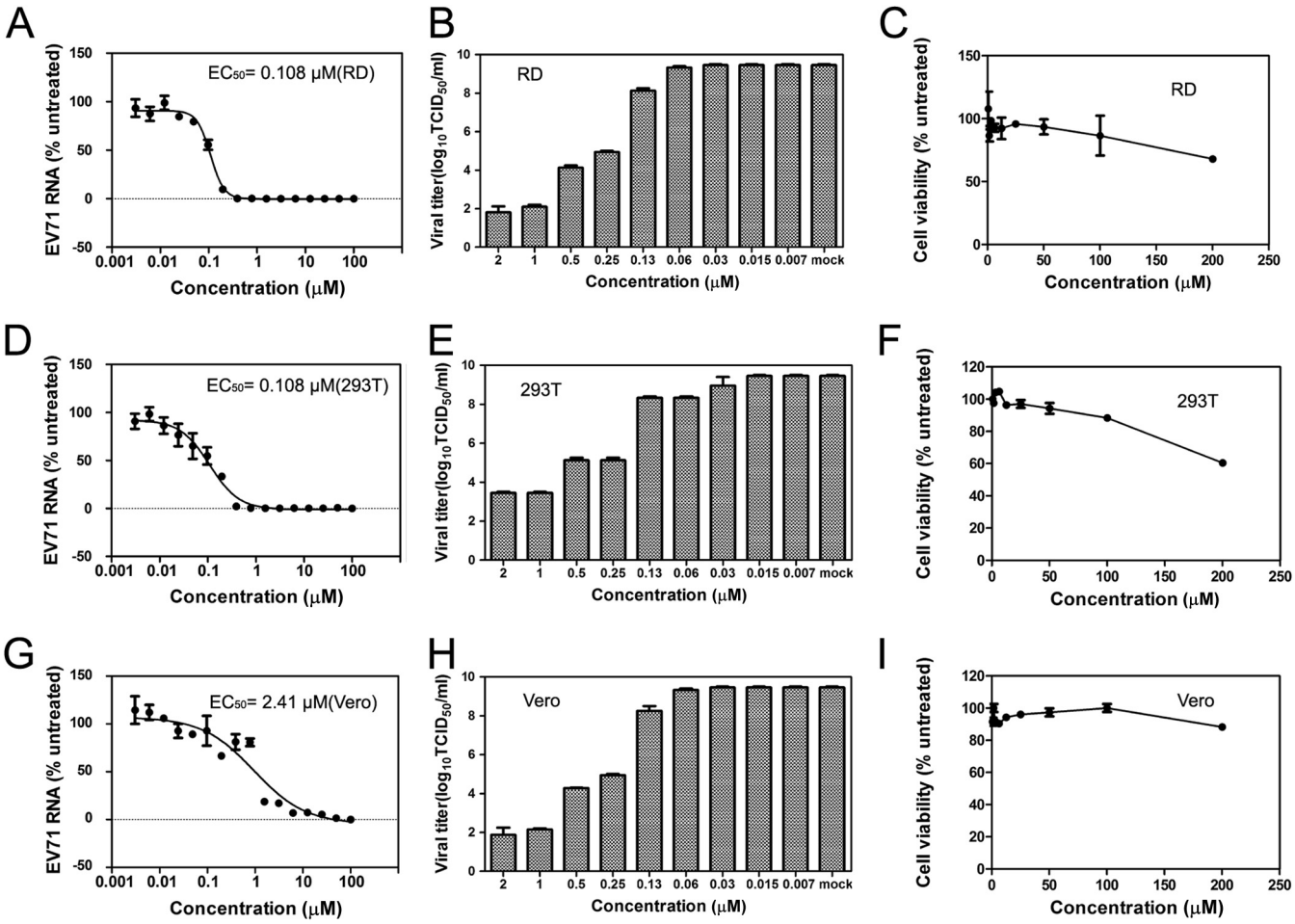

FIG 3 Quantification of anti-EV71 effect of NK-1.8k on different cell lines. (A, D, and G) RD, 293T, and Vero cells were treated with NK-1.8k and infected with EV71 strain Fuyang. EV71 RNA levels were measured by qRT-PCR at 24 hpi. (B, E, and H) RD, 293T, and Vero cells were treated with NK-1.8k and infected with EV71 strain Fuyang. The virus titers in the supernatants were determined at 72 hpi. (C, F, and I) Cytotoxicity in different cell lines. RD, 293T, and Vero cells were incubated with NK-1.8k at the indicated concentrations for 24 h. Cell viability was measured using a WST-1-based assay. Each point represents the average results from three independent experiments, and error bars represent SEMs ($n = 3$).

for the enzyme assay (33). The assays were performed with 100-μl samples containing 0.5 μM EV71 WT protease or the N69S or C147S mutant protease and 20 μM substrate in 50 mM Tris, pH 7.0, buffer. The enzymes were preincubated at 30°C for 30 min prior to the addition of the substrate. The reaction mixture was then incubated for 2 h at 30°C. The reaction was terminated by the addition of acetonitrile at 10-min intervals. The intensity of the OD for NMA and DNP was read at an excitation wavelength (λ_{ex}) of 340 nm and an emission wavelength (λ_{em}) of 440 nm.

RESULTS

NK-1.8k is an inhibitor of EV71 infection. Our aim in this work was to find an inhibitor that can inhibit the correct function of viral $3C^{pro}$ during the replication of EV71. A quick phenotype screening was performed using a total of 87 protease inhibitor derivatives that were initially assayed for their antiviral activity against EV71 by using RD cells infected with EV71 strain SK-EV006 that expressed GFP upon infection (34). Most of the tested compounds exhibited no obvious anti-EV71 effect at a concentration of 20 μM, and GFP expression remained obvious in infected RD cells. In contrast, treatment with a peptidyl aldehyde, NK-1.8k {*N*-[(*S*)-3-(4-fluorophenyl)-1-oxo-1-{(*S*)-1-oxo-3-[(*S*)-2-oxopiperidin-3-yl]propan-2-ylamino}propan-2-yl]-5-methylisoxazole-3-carboxamide} (Fig. 1A), achieved apparent reductions in the level of expression of the reporter GFP at a concentration of 0.09 μM (Fig. 1B). NK-1.8k was further shown to cause concentration-dependent protection against EV71 infection by measurement of the level of GFP expression (Fig. 1B).

NK-1.8k is a novel peptidomimetic compound which has structural characteristics that distinguish it from rupintrivir (21) (Fig. 1A). NK-1.8k features a six-member-ring lactam coupled with an aldehyde functional group, while rupintrivir has a five-member-ring lactam coupled with an α,β-unsaturated ester. Moreover, rupintrivir is considered a tripeptidic analogue, whereas NK-1.8k is similar to a dipeptide. These features indicate that NK-1.8k has better drug-like properties with a lower molecular weight and fewer hydrogen bond donors and acceptors than rupintrivir (35).

We thus further studied the anti-EV71 activity of NK-1.8k by infecting RD cells with EV71 strain SK-EV006. The infected cells were treated with various concentrations of NK-1.8k for 24 h, and the remaining levels of EV71 RNA in the cells were determined by

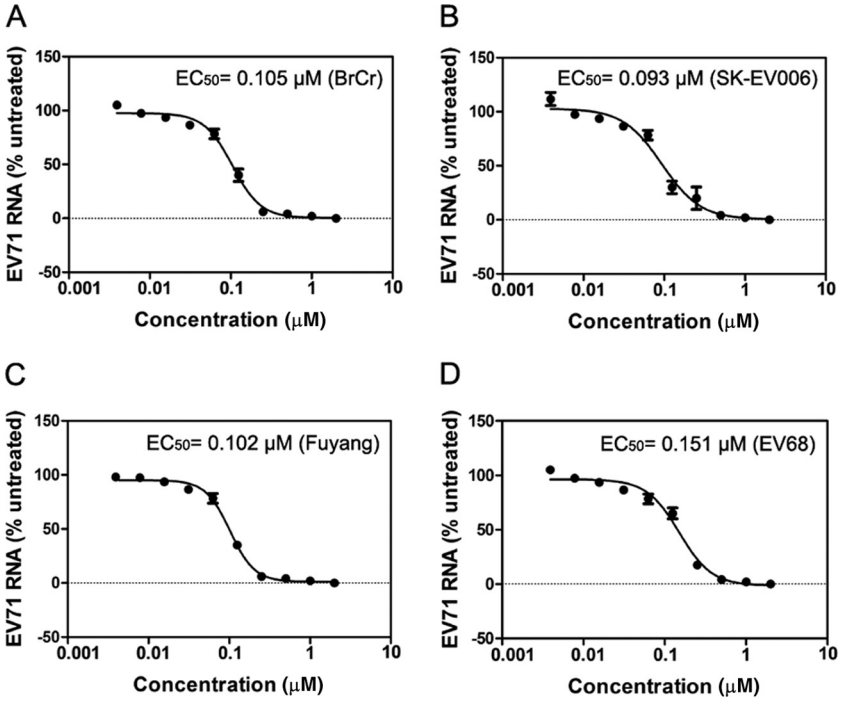

FIG 4 Quantification of antiviral effect of NK-1.8k on different virus strains. RD cells were treated with NK-1.8k and infected with living EV71 strain BrCr (genotype A) (A), EV71 strain SK-EV006 (genotype B) (B), EV71 strain Fuyang (genotype C) (C), and EV68 strain Fermon CA62-1 (D). The remaining levels of viral RNA in the cells were determined by the qRT-PCR method. Each point represents the average results from three independent experiments, and error bars represent SEMs ($n = 3$).

qRT-PCR. The results revealed that NK-1.8k showed a concentration-dependent reduction of EV71 RNA in infected cells with an EC_{50} of 34.5 nM (Fig. 1C). Moreover, it was observed that the expression of the VP1 protein of EV71 (the major component of the viral capsid) but not that of host GADPH, a host housekeeping gene, in the infected cells was also decreased by treatment with NK-1.8k (Fig. 1D). All these results support the possibility that NK-1.8k has an inhibitory effect on EV71 proliferation.

NK-1.8k impacts EV71 genome replication. Because NK-1.8k is potentially a protease inhibitor, we first analyzed whether NK-1.8k affects viral replication but not the entry process. A previously reported pseudotype EV71 system was used to exclude the possibility of an impact of virus reinfection (36).

We infected RD cells with EV71(FY)-Luc pseudotype virus and then treated the cells with NK-1.8k at a concentration of 0.2 μM, NITD008 (a reported polymerase inhibitor) (18, 19) at a concentration of 4 mM, and GPP3 (23) at a concentration of 1 pM at −6, −4, −2, 2, 4, 6, 8, and 10 hpi, in which 0 hpi indicates the time that the inhibitors were supplied immediately after virus infection. The results showed that the inhibition of EV71 by NK-1.8k had no dependence on treatment time before 10 hpi (Fig. 2A). The treatments with NK-1.8k at −6 to 8 hpi displayed the strongest antiviral effect, which is similar to the findings reported for the viral replication inhibitor NITD008 (Fig. 2B). In sharp contrast, the antiviral effect of GPP3 showed a dramatic decrease from 2 hpi (Fig. 2C).

We next directly transfected EV71 subgenomic replicon RNA lacking the P1 region into RD cells treated with NK-1.8k (0.2 μM), NITD008 (2 μM), and GPP3 (1 pM). The results showed that NK-1.8k caused the inhibition of EV71 replication to a level similar to the level of inhibition caused by NITD008 but distinctly different from that caused by GPP3 (Fig. 2D). Because this transfection excluded the region of the genome responsible for the entry step of viral infection, all of these results support the suggestion that NK-1.8k inhibits EV71 proliferation by affecting the viral replication stage.

Quantification of the anti-EV71 effect of NK-1.8k in different cell lines. To assess possible cell type- and species-dependent differences in the anti-EV71 activity of NK-1.8k, its antiviral effects in RD, 293T, and Vero cells were examined (Fig. 3).

The results revealed that NK-1.8k suppresses the viral RNA yield of EV71-infected RD, 293T, and Vero cells in a dose-dependent fashion. The EC_{50}s of NK-1.8k against EV71 SK-EV006 infection in RD, 293T, and Vero cells were determined to be 0.108, 0.108 and 2.41 μM, respectively (Fig. 3A, D, and G).

We also measured the reduction of virus titers after treatment with NK-1.8k in EV71-infected RD cells. Consistently, the results indicated that the virus titers in the supernatants were also significantly attenuated by treatment with NK-1.8k (Fig. 3B, E, and H).

The cytotoxicity of NK-1.8k for RD, 293T, and Vero cells was also tested. The results revealed that NK-1.8k at a high concentration of 200 μM has no obvious toxicity for any of the three cell lines (Fig. 3C, F, and I). Taken together, these results indicate that NK-1.8k inhibited EV71 with a high potency and the anti-EV71 activity of NK-1.8k has a high to satisfactory selectivity index (SI; where SI is equal to CC_{50}/EC_{50}, where CC_{50} is the 50% cytotoxic concentration) of up to 1,000 in RD cells.

NK-1.8k has a broad antiviral effect against multiple EV71 strains and EV68. EV71 is generally characterized as three genotypes, i.e., genotypes A, B, and C. We hypothesized that NK-1.8k

A

	location	3C
SelA	Nucleotide	AAC/AGC
	Amino acid	N69S
SelB	Nucleotide	AAC/AGC
	Amino acid	N69S
SelC	Nucleotide	AAC/AGC
	Amino acid	N69S

B

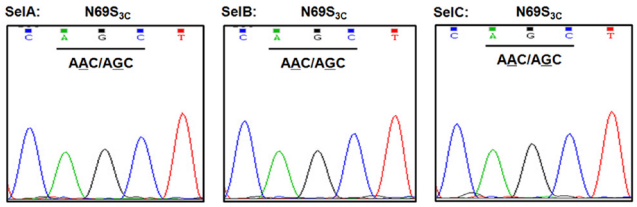

FIG 5 Mutation identified in NK-1.8k-resistant EV71. (A) Mutations recovered from resistant viruses were tabulated according to the amino acid positions and the corresponding protein. Sequencing of the complete genomes of 24 viruses from SelA, SelB, and SelC was performed. (B) Sequence chromatograms of the mutations found in resistant viruses. Representative sequencing chromatograms are presented for SelA, SelB, and SelC.

may have a broad antiviral effect against viruses of all three genotypes. Therefore, we infected RD cells with three different virus strains, including BrCr (genotype A), SK-EV006 (genotype B), and Fuyang (genotype C), treated them with NK-1.8k, and measured the remaining levels of EV71 RNA inside host cells through a qRT-PCR method. The results showed that NITD008 inhibited the viruses of strains BrCr, SK-EV006, and Fuyang with EC_{50}s of 0.105, 0.093, and 0.102 μM, respectively (Fig. 4A to C). Moreover, we also tested the antiviral effect of NK-1.8k on EV68 strain Fermon CA62-1 and found an EC_{50} of 0.151 μM against EV68 infection. All these results suggest that NK-1.8k has a broad range of inhibition and can inhibit different enteroviruses.

Selection and identification of resistant viruses. The NK-1.8k-resistant viruses were selected by continuously culturing EV71 for eight rounds in the presence of gradually increasing concentration of NK-1.8k: 0.2 μM (three rounds), 0.4 μM (three rounds), and 0.8 μM (two rounds). Three independent selections (SelA, SelB, and SelC) were performed to test the reproducibility of the resistance results.

Sequence analyses of the entire genomes of multiple resistant viruses identified a single A-to-G mutation at nucleotide position 5592 of the whole EV71 genome. This mutation translated into a single amino acid replacement of an asparagine residue by a serine residue at position 69 within the $3C^{pro}$ polypeptide (Fig. 5A and B). Because NK-1.8k was screened out of the library of compounds targeting the viral protease, this drug resistance is reasonable.

Sensitivity of WT EV71 and EV71 with the N69S mutation to NK-1.8k. We further examined the fitness and drug resistance of the N69S mutant virus. We first examined the effect of this mutation on viral replication in the absence of the compound. RD cells were transfected with equal amounts of WT EV71 or EV71 mutant N69S RNA and assayed for virus titers after transfection. The results revealed that the titer of the N69S mutant virus had an apparent decrease in comparison to that of the WT virus, suggesting that the fitness of the N69S mutant virus is inferior to that of the WT virus (Fig. 6A).

We next examined the sensitivity of mutant viruses to NK-1.8k

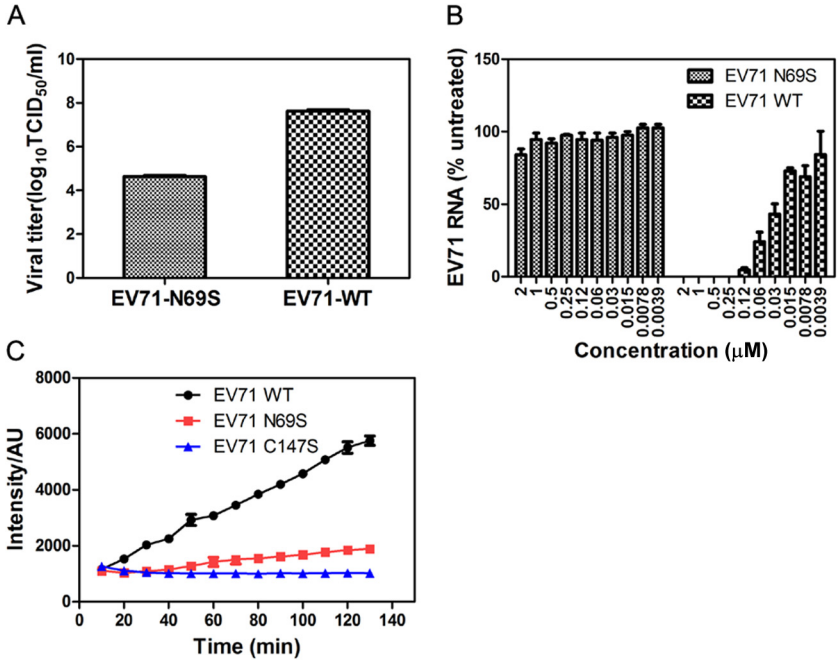

FIG 6 Sensitivity of WT EV71 and the N69S mutant virus to NK-1.8k. (A) Titers of EV71 WT and N69S mutant viruses. (B) RD cells were treated with NK-1.8k at concentrations ranging from 2 to 0.0039 μM and infected with the EV71 WT or N69S mutant at an MOI of 1. The inhibitory activities were determined by qRT-PCR. (C) Protease activity of EV71 WT, the N69S mutant, and the C147S mutant. The intensities of the ODs for EV71 WT, N69S mutant, and C147S mutant proteases were read at a λ_{ex} of 340 nm and a λ_{em} of 440 nm every 10 min for 120 min. AU, absorbance units.

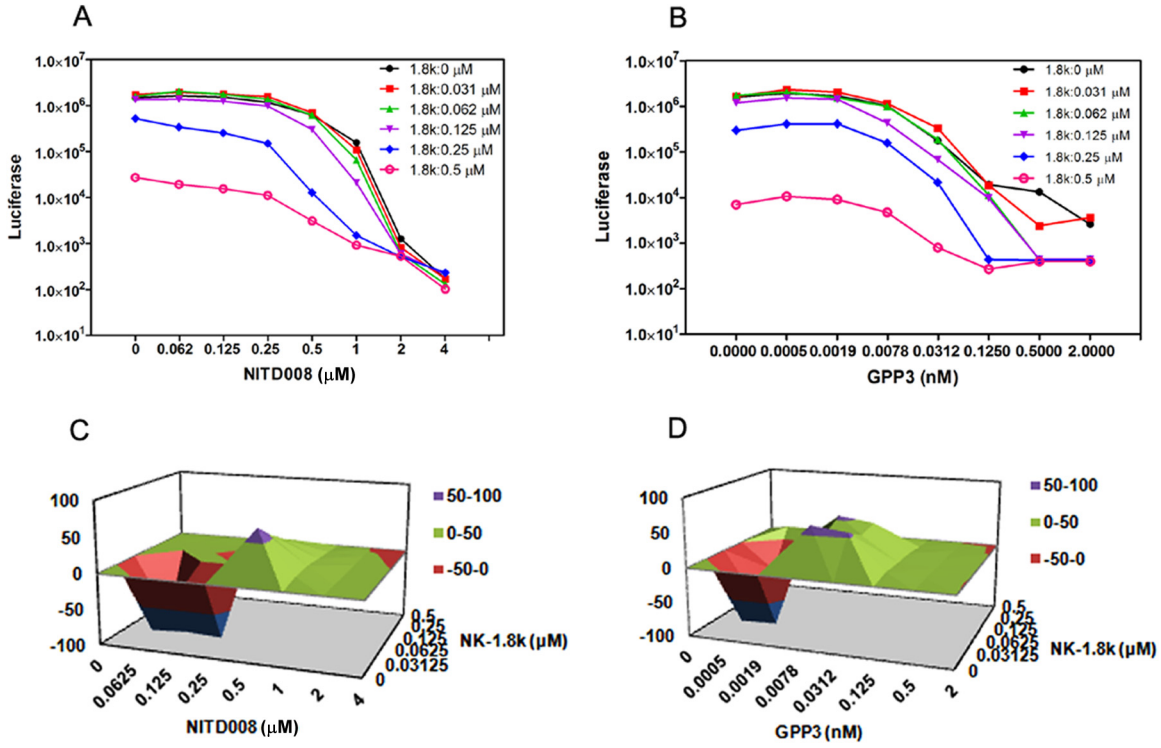

FIG 7 Interaction of NK-1.8k with other inhibitors of EV71 proliferation. (A and B) Anti-EV71 effects of the combinations NK-1.8k plus NITD008 and NK-1.8k plus GPP3. (C and D) Differential surface plots at the 95% confidence interval (CI) were calculated and generated by using the MacSynergy II program for the interactions of the combinations NK-1.8k plus NITD008 (C) and NK-1.8k plus GPP3 (D). The *y* axes show the volumes of synergy or antagonism (in mM^2%).

inhibition using a qRT-PCR assay. The results showed that the N69S mutation conferred complete resistance to NK-1.8k, but the WT virus did not show any resistance (Fig. 6B). Collectively, all these results demonstrate that the N69S mutation attenuates the fitness of virus growth but helps the virus to escape inhibition by NK-1.8k.

Protease activities of WT and N69S mutant $3C^{pro}$. In order to verify the influence of the EV71 N69S amino acid substitution on enzyme activity, the peptide NMA-IEALFQGPPK(DNP)FR was used as the substrate for the protease assay. The OD intensity was read at an λ_{ex} of 340 nm and an λ_{em} of 440 nm every 10 min.

The results determined from the change in the intensity of the OD within 120 min of exposure demonstrated that the $3C^{pro}$ protease with the N69S mutation retained a low level of protease activity compared to that of the catalytically defective mutant with the C147S mutation but that its protease activity was much lower than that of WT $3C^{pro}$ (Fig. 6C). This is consistent with the lower fitness of the virus with the N69S mutation.

Effects of the combination of NK-1.8k and polymerase and entry inhibitors against EV71 infection. The use of therapies with combinations of drugs with different mechanisms of action has been proven to be an effective approach to the treatment of viral infections, including HIV and hepatitis C virus infections. We reasoned that the use of a combination of entry and polymerase inhibitors of EV71 with NK-1.8k might offer benefits over the use of each single monotherapy. To test this hypothesis, we measured the inhibition of EV71 propagation by NITD008 and GPP3 in combination with NK-1.8k.

The combinations of NK-1.8k with NITD008 and with GPP3 were evaluated with the single-round pseudotype EV71 reporter system. The results revealed a concentration-dependent inhibition of EV71 replication by NK-1.8k, NITD008, or GPP3 alone or with any two of these drugs in combination. The combinations of NK-1.8k plus NITD008 (Fig. 7A) and NK-1.8k plus GPP3 (Fig. 7B) at various concentrations resulted in inhibition greater than that achieved with either compound in the combination alone.

The data were further analyzed using a mathematical model, MacSynergy II, to determine whether the effect of the combinations was synergistic, additive, or antagonistic. The results revealed that the combination of NK-1.8k and NITD008 had antiviral effects that were significantly more potent than the theoretical additive effects above concentrations of 0.25 μM for NITD008 and 1.9 pM for GPP3. This finding supports the suggestion that this combination is indeed synergistic (Fig. 7C and D). Because the effects of NK-1.8k, NITD008, and GPP3 on cell viability were previously evaluated to ensure that the inhibition of EV71 was not due to cytotoxicity, it is not surprising that no significant cytotoxicity was observed with the combination of NK-1.8k and either of the other two compounds (data not shown). Therefore, the observed synergy is indeed specific and does not reflect synergistic toxicity.

DISCUSSION

All picornaviruses, such as EV71, polioviruses, rhinoviruses (RVs), CVs, and hepatitis A virus, encode a cysteine protease (named $3C^{pro}$) that proteolytically processes the polyprotein into functional viral proteins (37). Because the viral protease has strict substrate specificity and lacks homologues in mammalian cells, it

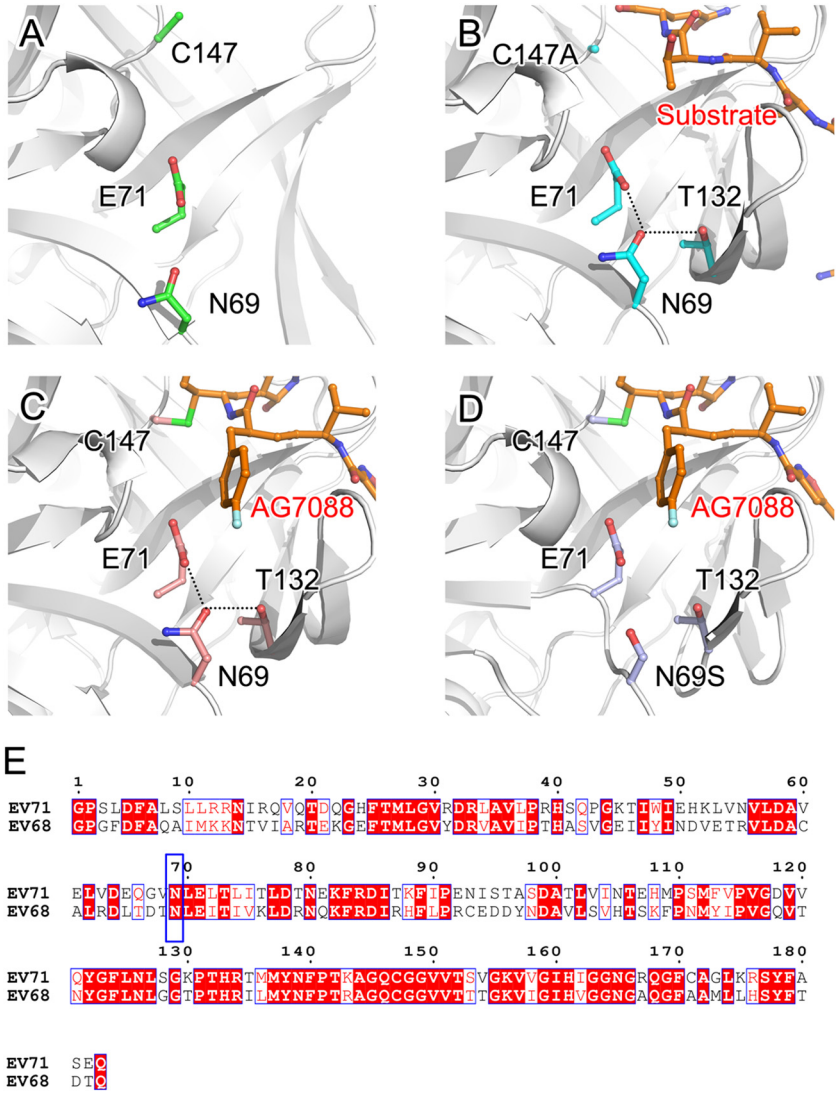

FIG 8 N69S may alter the conformation of the active site of EV71 3C^{pro}. The structures of WT EV71 3C^{pro} (PDB accession number 3OSY) (A), the catalytically defective C147A mutant of CVA16 3C^{pro} in complex with a substrate peptide (PDB accession number 3SJ9) (B), EV71 3C^{pro} in complex with rupintrivir (AG7088; PDB accession number 3SJO) (C), and a modeled structure of EV71 3C^{pro} with the N69S mutant (D) were aligned and are presented in the same orientation. The polypeptides of protease are shown as white cartoon diagrams; the substrate peptide and rupintrivir (AG7088) molecule are displayed as stick models. Key residues N69 (or N69S), E71, T132, and C147 are also represented as colored sticks. The hydrogen bonds between the side chains of N69 and E71/T132 are denoted as dashed lines. (E) Sequence alignment of EV71 strain Fuyang and EV68 strain Fermon CA62-1. The strictly conserved residues are shown as white text with a red background, whereas the conserved residues are displayed as red text with a white background. The blue frame highlights drug resistance-conferring residue N69.

is recognized to be the most essential target, together with viral polymerase, for antiviral discovery (38). Therefore, we systematically analyzed the substrate specificity of virus-encoded cysteine proteases and generated a chemical compound library targeting viral cysteine protease activity through a combinational chemistry method.

In this study, by screening the compounds in our protease-targeted library, we verified that a peptidyl aldehyde, NK-1.8k, targets the EV71 protease to inhibit the replication of various virus strains. NK-1.8k has no obvious cytotoxicity, even at a high concentration of 200 μM, for different cell lines. Through the screening of drug-resistant viruses, we identified the amino acid substitution N69S on the EV71 protease to be the substitution that confers resistance. Although this substitution attenuated the protease activity of 3C^{pro} and the fitness of EV71, it helped the virus to completely escape from NK-1.8k treatment, supporting the suggestion that NK-1.8k directly inhibits the activity of viral protease itself.

A previous study identified several mutations in human rhinoviruses (HRVs) that confer resistance to treatment with rupintrivir, including the T129/130, T131, T143, N165, N130, and L136 mutations (39). By checking the crystal structure of EV71 3C^{pro} (40), the N69S substitution unexpectedly appears to be close to but outside the active site of EV71 3C^{pro} (Fig. 8), which differs from the sites of the rupintrivir resistance-conferring mutations in HRV. The side chain of the N69 residue contacts with nearby

residues E71 and T132 via hydrogen bonds and stabilizes the conformation of the active site of EV71 $3C^{pro}$ when the substrate peptide or AG7088 inhibitor binds to $3C^{pro}$ (Fig. 8B and C). The replacement of the residue at this position by a serine residue shortens the side chain and would abolish these contacts (Fig. 8D). Interestingly, previous crystallographic work has found that the side chain of N69 forms an essential hydrogen bond with catalytic residue E71 to stabilize the catalytic triad, and biochemical analysis demonstrated that the interruption of this hydrogen bond by an N-to-S replacement significantly reduces the K_m/k_{cat} values of EV71 $3C^{pro}$ (40). We therefore propose that this amino acid substitution accommodates the higher structural flexibility of the active site of $3C^{pro}$ and allows polypeptide binding in the $3C^{pro}$ active site in the presence of the inhibitor NK-1.8k. Since the residues constituting the active site of $3C^{pro}$ and the N69 residue are strictly conserved between EV71 and EV68 strains (Fig. 8E), it is conceivable that NK-1.8k has a consistent mechanism of inhibition of these two viruses. Determination of the complex crystal structures of NK-1.8k and WT $3C^{pro}$ and of the natural substrate and N69S $3C^{pro}$ is warranted to dissect the precise role of N69 in the function of $3C^{pro}$.

ACKNOWLEDGMENTS

This work is supported by the National Major Project (973 Program) (grant no. 2014CB542800 and 2013CB911100), the National Natural Science Foundation of China (grant no. 81330036, 81322023, 31370733, and 31170678), and the Tsinghua University Initiative Scientific Research Program (grant no. 20141080146 and 20131089228).

REFERENCES

1. **Wang Y, Qing J, Sun Y, Rao Z.** 2014. Suramin inhibits EV71 infection. Antiviral Res **103:**1–6. http://dx.doi.org/10.1016/j.antiviral.2013.12.008.
2. **Chen CY, Chang YC, Huang CC, Lui CC, Lee KW, Huang SC.** 2001. Acute flaccid paralysis in infants and young children with enterovirus 71 infection: MR imaging findings and clinical correlates. Am J Neuroradiol **22:**200–205.
3. **Wang Y, Feng Z, Yang Y, Self S, Gao Y, Longini IM, Wakefield J, Zhang J, Wang L, Chen X, Yao L, Stanaway JD, Wang Z, Yang W.** 2011. Hand, foot, and mouth disease in China: patterns of spread and transmissibility. Epidemiology **22:**781–792. http://dx.doi.org/10.1097/EDE.0b013e318231d67a.
4. **Stewart CL, Chu EY, Introcaso CE, Schaffer A, James WD.** 2013. Coxsackievirus A6-induced hand-foot-mouth disease. JAMA Dermatol **149:**1419–1421. http://dx.doi.org/10.1001/jamadermatol.2013.6777.
5. **Yang Y, Wang H, Gong E, Du J, Zhao X, McNutt MA, Wang S, Zhong Y, Gao Z, Zheng J.** 2009. Neuropathology in 2 cases of fatal enterovirus type 71 infection from a recent epidemic in the People's Republic of China: a histopathologic, immunohistochemical, and reverse transcription polymerase chain reaction study. Hum Pathol **40:**1288–1295. http://dx.doi.org/10.1016/j.humpath.2009.01.015.
6. **Zhang Y, Zhu Z, Yang W, Ren J, Tan X, Wang Y, Mao N, Xu S, Zhu S, Cui A, Zhang Y, Yan D, Li Q, Dong X, Zhang J, Zhao Y, Wan J, Feng Z, Sun J, Wang S, Li D, Xu W.** 2010. An emerging recombinant human enterovirus 71 responsible for the 2008 outbreak of hand foot and mouth disease in Fuyang City of China. Virol J **7:**94. http://dx.doi.org/10.1186/1743-422X-7-94.
7. **Kreuter JD, Barnes A, McCarthy JE, Schwartzman JD, Oberste MS, Rhodes CH, Modlin JF, Wright PF.** 2011. A fatal central nervous system enterovirus 68 infection. Arch Pathol Lab Med **135:**793–796. http://dx.doi.org/10.1043/2010-0174-CR.1.
8. **Tokarz R, Firth C, Madhi SA, Howie SR, Wu W, Sall AA, Haq S, Briese T, Lipkin WI.** 2012. Worldwide emergence of multiple clades of enterovirus 68. J Gen Virol **93:**1952–1958. http://dx.doi.org/10.1099/vir.0.043935-0.
9. **Sun Y, Wang Y, Shan C, Chen C, Xu P, Song M, Zhou H, Yang C, Xu W, Shi PY, Zhang B, Lou Z.** 2012. Enterovirus 71 VPg uridylation uses a two-molecular mechanism of 3D polymerase. J Virol **86:**13662–13671. http://dx.doi.org/10.1128/JVI.01712-12.
10. **McMinn PC.** 2002. An overview of the evolution of enterovirus 71 and its clinical and public health significance. FEMS Microbiol Rev **26:**91–107. http://dx.doi.org/10.1111/j.1574-6976.2002.tb00601.x.
11. **Gamarnik AV, Andino R.** 1998. Switch from translation to RNA replication in a positive-stranded RNA virus. Genes Dev **12:**2293–2304. http://dx.doi.org/10.1101/gad.12.15.2293.
12. **Hillman BI, Foglia R, Yuan W.** 2000. Satellite and defective RNAs of Cryphonectria hypovirus 3-Grand Haven 2, a virus species in the family Hypoviridae with a single open reading frame. Virology **276:**181–189. http://dx.doi.org/10.1006/viro.2000.0548.
13. **Pelletier J, Sonenberg N.** 1988. Internal initiation of translation of eukaryotic mRNA directed by a sequence derived from poliovirus RNA. Nature **334:**320–325. http://dx.doi.org/10.1038/334320a0.
14. **Chen C, Wang Y, Shan C, Sun Y, Xu P, Zhou H, Yang C, Shi PY, Rao Z, Zhang B, Lou Z.** 2013. Crystal structure of enterovirus 71 RNA-dependent RNA polymerase complexed with its protein primer VPg: implication for a *trans* mechanism of VPg uridylylation. J Virol **87:**5755–5768. http://dx.doi.org/10.1128/JVI.02733-12.
15. **Sun Y, Guo Y, Lou Z.** 2014. Formation and working mechanism of the picornavirus VPg uridylylation complex. Curr Opin Virol **9:**24–30. http://dx.doi.org/10.1016/j.coviro.2014.09.003.
16. **Zhu FC, Liang ZL, Li XL, Ge HM, Meng FY, Mao QY, Zhang YT, Hu YM, Zhang ZY, Li JX, Gao F, Chen QH, Zhu QY, Chu K, Wu X, Yao X, Guo HJ, Chen XQ, Liu P, Dong YY, Li FX, Shen XL, Wang JZ.** 2013. Immunogenicity and safety of an enterovirus 71 vaccine in healthy Chinese children and infants: a randomised, double-blind, placebo-controlled phase 2 clinical trial. Lancet **381:**1037–1045. http://dx.doi.org/10.1016/S0140-6736(12)61764-4.
17. **Shang L, Xu M, Yin Z.** 2013. Antiviral drug discovery for the treatment of enterovirus 71 infections. Antiviral Res **97:**183–194. http://dx.doi.org/10.1016/j.antiviral.2012.12.005.
18. **Deng CL, Yeo H, Ye HQ, Liu SQ, Shang BD, Gong P, Alonso S, Shi PY, Zhang B.** 2014. Inhibition of enterovirus 71 by adenosine analog NITD008. J Virol **88:**11915–11923. http://dx.doi.org/10.1128/JVI.01207-14.
19. **Shang L, Wang Y, Qing J, Shu B, Cao L, Lou Z, Gong P, Sun Y, Yin Z.** 2014. An adenosine nucleoside analogue NITD008 inhibits EV71 proliferation. Antiviral Res **112:**47–58. http://dx.doi.org/10.1016/j.antiviral.2014.10.009.
20. **Dragovich PS, Prins TJ, Zhou R, Johnson TO, Brown EL, Maldonado FC, Fuhrman SA, Zalman LS, Patick AK, Matthews DA, Hou X, Meador JW, Ferre RA, Worland ST.** 2002. Structure-based design, synthesis, and biological evaluation of irreversible human rhinovirus 3C protease inhibitors. Part 7. Structure-activity studies of bicyclic 2-pyridone-containing peptidomimetics. Bioorg Med Chem Lett **12:**733–738. http://dx.doi.org/10.1016/S0960-894X(02)00008-2.
21. **Matthews DA, Dragovich PS, Webber SE, Fuhrman SA, Patick AK, Zalman LS, Hendrickson TF, Love RA, Prins TJ, Marakovits JT, Zhou R, Tikhe J, Ford CE, Meador JW, Ferre RA, Brown EL, Binford SL, Brothers MA, DeLisle DM, Worland ST.** 1999. Structure-assisted design of mechanism-based irreversible inhibitors of human rhinovirus 3C protease with potent antiviral activity against multiple rhinovirus serotypes. Proc Natl Acad Sci U S A **96:**11000–11007. http://dx.doi.org/10.1073/pnas.96.20.11000.
22. **Tijsma A, Franco D, Tucker S, Hilgenfeld R, Froeyen M, Leyssen P, Neyts J.** 2014. The capsid binder vapendavir and the novel protease inhibitor SG85 inhibit enterovirus 71 replication. Antimicrob Agents Chemother **58:**6990–6992. http://dx.doi.org/10.1128/AAC.03328-14.
23. **De Colibus L, Wang X, Spyrou JA, Kelly J, Ren J, Grimes J, Puerstinger G, Stonehouse N, Walter TS, Hu Z, Wang J, Li X, Peng W, Rowlands DJ, Fry EE, Rao Z, Stuart DI.** 2014. More-powerful virus inhibitors from structure-based analysis of HEV71 capsid-binding molecules. Nat Struct Mol Biol **21:**282–288. http://dx.doi.org/10.1038/nsmb.2769.
24. **Qing J, Wang Y, Sun Y, Huang J, Yan W, Wang J, Su D, Ni C, Li J, Rao Z, Liu L, Lou Z.** 2014. Cyclophilin A associates with enterovirus-71 virus capsid and plays an essential role in viral infection as an uncoating regulator. PLoS Pathog **10:**e1004422. http://dx.doi.org/10.1371/journal.ppat.1004422.
25. **Yin Z, Chen YL, Schul W, Wang QY, Gu F, Duraiswamy J, Kondreddi RR, Niyomrattanakit P, Lakshminarayana SB, Goh A, Xu HY, Liu W, Liu B, Lim JY, Ng CY, Qing M, Lim CC, Yip A, Wang G, Chan WL, Tan HP, Lin K, Zhang B, Zou G, Bernard KA, Garrett C, Beltz K, Dong M, Weaver M, He H, Pichota A, Dartois V, Keller TH, Shi PY.** 2009. An

adenosine nucleoside inhibitor of dengue virus. Proc Natl Acad Sci U S A **106:**20435–20439. http://dx.doi.org/10.1073/pnas.0907010106.

26. **Arita M, Wakita T, Shimizu H.** 2008. Characterization of pharmacologically active compounds that inhibit poliovirus and enterovirus 71 infectivity. J Gen Virol **89:**2518–2530. http://dx.doi.org/10.1099/vir.0.2008/002915-0.
27. **Prichard MN, Shipman C, Jr.** 1996. Analysis of combinations of antiviral drugs and design of effective multidrug therapies. Antivir Ther **1:**9–20.
28. **Prichard MN, Shipman C, Jr.** 1990. A three-dimensional model to analyze drug-drug interactions. Antiviral Res **14:**181–205. http://dx.doi.org/10.1016/0166-3542(90)90001-N.
29. **Cui S, Wang J, Fan T, Qin B, Guo L, Lei X, Wang J, Wang M, Jin Q.** 2011. Crystal structure of human enterovirus 71 3C protease. J Mol Biol **408:**449–461. http://dx.doi.org/10.1016/j.jmb.2011.03.007.
30. **Guo Y, Wang W, Ji W, Deng M, Sun Y, Zhou H, Yang C, Deng F, Wang H, Hu Z, Lou Z, Rao Z.** 2012. Crimean-Congo hemorrhagic fever virus nucleoprotein reveals endonuclease activity in bunyaviruses. Proc Natl Acad Sci U S A **109:**5046–5051. http://dx.doi.org/10.1073/pnas.1200808109.
31. **Li B, Wang Q, Pan X, Fernandez de Castro I, Sun Y, Guo Y, Tao X, Risco C, Sui SF, Lou Z.** 2013. Bunyamwera virus possesses a distinct nucleocapsid protein to facilitate genome encapsidation. Proc Natl Acad Sci U S A **110:**9048–9053. http://dx.doi.org/10.1073/pnas.1222552110.
32. **Zhou H, Sun Y, Guo Y, Lou Z.** 2013. Structural perspective on the formation of ribonucleoprotein complex in negative-sense single-stranded RNA viruses. Trends Microbiol **21:**475–484. http://dx.doi.org/10.1016/j.tim.2013.07.006.
33. **Shang L, Zhang S, Yang X, Sun J, Li L, Cui Z, He Q, Guo Y, Sun Y, Yin Z.** 24 November 2014. Biochemical characterization of recombinant enterovirus 71 3C protease with fluorogenic model peptide substrates and development of a biochemical assay. Antimicrob Agents Chemother http://dx.doi.org/10.1128/AAC.04698-14.
34. **Yamayoshi S, Yamashita Y, Li J, Hanagata N, Minowa T, Takemura T, Koike S.** 2009. Scavenger receptor B2 is a cellular receptor for enterovirus 71. Nat Med **15:**798–801. http://dx.doi.org/10.1038/nm.1992.
35. **Lipinski CA, Lombardo F, Dominy BW, Feeney PJ.** 2001. Experimental and computational approaches to estimate solubility and permeability in drug discovery and development settings. Adv Drug Deliv Rev **46:**3–26. http://dx.doi.org/10.1016/S0169-409X(00)00129-0.
36. **Chen P, Song Z, Qi Y, Feng X, Xu N, Sun Y, Wu X, Yao X, Mao Q, Li X, Dong W, Wan X, Huang N, Shen X, Liang Z, Li W.** 2012. Molecular determinants of enterovirus 71 viral entry: cleft around GLN-172 on VP1 protein interacts with variable region on scavenge receptor B 2. J Biol Chem **287:**6406–6420. http://dx.doi.org/10.1074/jbc.M111.301622.
37. **Kuo CJ, Shie JJ, Fang JM, Yen GR, Hsu JT, Liu HG, Tseng SN, Chang SC, Lee CY, Shih SR, Liang PH.** 2008. Design, synthesis, and evaluation of 3C protease inhibitors as anti-enterovirus 71 agents. Bioorg Med Chem **16:**7388–7398. http://dx.doi.org/10.1016/j.bmc.2008.06.015.
38. **Lou Z, Sun Y, Rao Z.** 2014. Current progress in antiviral strategies. Trends Pharmacol Sci **35:**86–102. http://dx.doi.org/10.1016/j.tips.2013.11.006.
39. **Binford SL, Weady PT, Maldonado F, Brothers MA, Matthews DA, Patick AK.** 2007. In vitro resistance study of rupintrivir, a novel inhibitor of human rhinovirus 3C protease. Antimicrob Agents Chemother **51:**4366–4373. http://dx.doi.org/10.1128/AAC.00905-07.
40. **Wang J, Fan T, Yao X, Wu Z, Guo L, Lei X, Wang J, Wang M, Jin Q, Cui S.** 2011. Crystal structures of enterovirus 71 3C protease complexed with rupintrivir reveal the roles of catalytically important residues. J Virol **85:**10021–10030. http://dx.doi.org/10.1128/JVI.05107-11.